UVicSPACE: Research & Learning Repository

University of Victoria

Faculty of Science

Faculty Publications

This is a post-review version of the following article:

Seafloor weathering and the oxygen isotope ratio in seawater: Insight from whole-rock δ^{18} O and carbonate δ^{18} O and Δ_{47} from the Troodos ophiolite

L.A. Coogan, M. Daëron, K.M. Gillis

February 2019

The final publication will be available at:

https://doi.org/10.1016/j.epsl.2018.12.014

Citation for this paper:

Coogan, L.A., Daëron, M. & Gillis, K.M. (2019). Seafloor weathering and the oxygen isotope ratio in seawater: Insight from whole-rock δ^{18} O and carbonate δ^{18} O and Δ_{47} from the Troodos ophiolite. *Earth and Planetary Science Letters, 508,* 41-50. https://doi.org/10.1016/j.epsl.2018.12.014

Seafloor weathering and the oxygen isotope ratio in seawater: insight from whole-rock $\delta^{18}O$ and carbonate $\delta^{18}O$ and Δ_{47} from the Troodos ophiolite

[1*]L.A. Coogan, [2]M. Daëron and [1]K.M. Gillis

[1]School of Earth and Ocean Sciences, University of Victoria, Victoria, Canada, V8P 5C2

[2]CNRS/LSCE, Batiment 12 - Avenue de la Terrasse, 91198 Gif-sur-Yvette, France

*corresponding author: lacoogan@uvic.ca

Coogan, L.A., Daëron, M., Gillis, K.M., 2019. Seafloor weathering and the oxygen isotope ratio in seawater: Insight from whole-rock δ18O and carbonate δ18O and Δ47 from the Troodos ophiolite. Earth Planet. Sci. Lett. 508, 41–50.

Abstract

The controls on, and history of, the oxygen isotope ratio in seawater continue to be debated after many decades of research with the lack of consensus in large part reflecting uncertainty in the role of hydrothermal exchange between seawater and the oceanic crust. We have investigated this using new carbonate Δ_{47} and $\delta^{18}O$ data, and whole-rock O-isotope data, for samples from the lava section of the Troodos ophiolite. Carbonate data confirm that fluid-to-rock ratios in the upper lavas during off-axis hydrothermal circulation are generally sufficiently large that both the fluid $\delta^{18}O$ and

temperature are similar to those of bottom water. However, some samples require more complicated interpretations that could reflect changes in the rate of calcite formation. Whole-rock data indicate that O-isotope exchange in the lavas is directly linked to the major element exchange that leads to alkalinity production (i.e., CO_2 consumption) and both are dependent on bottom water temperature. This means that the O-isotopic composition of seawater is linked to the long-term C-cycle. The data are used to parameterize a simple model of the evolution of the O-isotopic composition of seawater driven by changes in solid earth CO_2 degassing. Alkalinity balance links the total extent of weathering of the continents and seafloor, which are sinks for high $\delta^{18}O$ material, to CO_2 degassing rate and surface temperature. The modelling suggests that if solid earth CO_2 degassing and the rate of formation of oceanic crust are linked, the O-isotopic composition of the ocean (including any ice sheets) is unlikely to have varied more than ±1‰ over the Phanerozoic.

1. Introduction

The oxygen isotope composition of seawater ($\delta^{18}O_{SW}$) provides important insight into the fluid-rock interactions, both on the continents and at the bottom of the oceans, that control important aspects of ocean chemistry (e.g. Muehlenbachs and Clayton, 1976; Jaffrés et al., 2007). Continental weathering leads to O-isotope fractionation between the weathering products and associated fluids that ultimately return to the ocean (e.g. Savin and Epstein, 1970). Likewise, seafloor hydrothermal systems fractionate O-isotopes between the secondary minerals and modified seawater (Gregory and Taylor, 1981; Alt et al., 1986). Precipitation of chemical sediments and diagenetic phases are also associated with O-isotope fractionation. Because the processes that control the O-isotopic composition of the ocean are important for many long-term element cycles in the ocean, a quantitative understanding of the controls on the O-isotope composition of seawater, and how this has changed over Earth history, is of fundamental importance to our understanding of the Earth system.

Despite decades of research there is an ongoing controversy about whether $\delta^{18}O_{SW}$ has changed substantially, or remained almost constant, over Earth history. On one hand, the $\delta^{18}O$ of carbonates and cherts are generally isotopically lighter the older they are (Perry, 1967; Fritz, 1971), with early Phanerozoic and Archean carbonates ~6 to 8‰ and ~15‰ lighter than modern carbonates, respectively (e.g. Veizer and Prokoph, 2015; Shields and Viezer, 2002; Jaffrés et al., 2007). This has been interpreted as indicating similarly light palaeoseawater (Perry, 1967; Walker and Lohmann, 1989; Veizer et al., 1999; Wallmann, 2004; Kasting et al., 2006; Jaffrés et al., 2007; Veizer and

Prokoph, 2015). Alternatively, it has been argued that the formation of low $\delta^{18}O$ secondary minerals in high-temperature, on-axis, seafloor hydrothermal systems, and high ^{18}O secondary minerals in low-temperature, off-axis, seafloor hydrothermal systems tends to force $\delta^{18}O_{SW}$ towards being ~6‰ lighter than oceanic crust (e.g. Muehlenbachs, 1998). Since the $\delta^{18}O$ of the mantle has remained almost constant over time, the implication of this model is that the same must be true for seawater (Muehlenbachs and Clayton, 1976; Gregory and Taylor, 1981; Muehlenbachs, 1998; Turchyn et al., 2013). Recently, clumped isotope measurements of sedimentary carbonates have provided independent evidence that $\delta^{18}O_{SW}$ has not changed substantially over the Phanerozoic (Came et al., 2007; Cummins et al., 2014; Finnegan et al., 2011; Henkes et al., 2018; Ryb and Eiler, 2018) however the interpretation of these data have been questioned (Veizer and Prokoph, 2015). Resolutions to this controversy range from explaining the carbonate and chert $\delta^{18}O$ record as reflecting high paleoseawater temperatures and/or post-depositional modification through to postulating significant changes in how oceanic hydrothermal systems operate (e.g. Muehlenbachs, 1998; Gregory and Taylor, 1981; Kasting et al., 2006; Jaffrés et al., 2007).

Irrespective of whether authors conclude that $\delta^{18}O_{SW}$ has remained nearly constant or changed dramatically, it is generally accepted that oceanic hydrothermal processes are key in controlling $\delta^{18}O_{SW}$ (e.g. Muehlenbachs, 1998; Lécuyer and Allemand, 1999; Gregory and Taylor, 1981; Kasting et al., 2006; Jaffrés et al., 2007). A number of recent studies have suggested that $\delta^{18}O_{SW}$ increased ~6‰ over the Phanerozoic and that this was largely due to a decrease in the extent of low-temperature alteration of the upper oceanic crust (Wallmann, 2004; Kasting et al., 2006; Jaffrés et al.,

2007). In this model increased abyssal sedimentation starting in the early Phanerozoic is hypothesized to have reduced the extent of off-axis hydrothermal alteration of the lavas decreasing the magnitude of this high $\delta^{18}O$ sink. Here we present new carbonate (Δ_{47} and $\delta^{18}O$) and whole-rock ($\delta^{18}O$) analyses of seafloor lavas from the Troodos ophiolite. These data, along with compiled data, are used to guide the construction and calibration of a simple model of the controls on $\delta^{18}O_{SW}$. The model shows that coupling between the C-cycle and $\delta^{18}O_{SW}$ make a 6-8‰ change in $\delta^{18}O_{SW}$ over the Phanerozoic unlikely.

2. Oxygen isotope exchange between the ocean and the oceanic crust

Oxygen-isotope exchange between the ocean and oceanic crust occurs under very different conditions in on- and off-axis regions (Fig. 1). On-axis hydrothermal circulation is driven by the cooling of magma chambers and plutonic rocks, with larger fluid fluxes in the higher permeability dikes than in the underlying, lower permeability, plutonic rocks. Temperatures of fluid-rock interaction in the dikes and plutonic rocks are typically 350-750°C leading to the formation of secondary minerals that are predicted to have $^{18}O/^{16}O$ ratios similar to that of the fluid they grew from ($1000\ln(\alpha_{r/w}) \sim 0\pm2$‰, where $\alpha_{r/w}$ is the $^{18}O/^{16}O$ fractionation factor between rock and water). High-temperatures and hydrous conditions are expected to lead to a close approach to equilibrium O-isotope exchange. This means that for the modern system the $\delta^{18}O$ of dikes and plutonic rocks (initial $\delta^{18}O_{SMOW}$ ~5.7‰) decrease slightly during on-axis, high-temperature, hydrothermal alteration (Fig. 2; Alt et al., 1986; Gregory and Taylor, 1981). The average dike from the modern ocean basin ($\delta^{18}O_{SMOW}$ = 4.5‰; standard error = 0.06; n = 219) is slightly isotopically lighter than the average plutonic rock ($\delta^{18}O_{SMOW}$ = 5.1‰; standard

error = 0.08; n = 315), largely because the higher permeability in the dikes leads to higher water-to-rock ratios (~1 versus <1; e.g., Alt et al., 1986; Kirchner and Gillis, 2012). A more limited dataset from the Troodos ophiolite gives a very similar result (Fig. 2), consistent with high-temperature alteration of the dikes and plutonics operating under similar conditions as in modern crust.

Fluid-flow in the off-axis is driven by the cooling of the oceanic lithosphere and is focused in the high permeability lavas (upper ~500 m of the crust) where water-to-rock ratios are about three orders of magnitude higher than in on-axis systems (Fig. 1; e.g., Coogan and Gillis, 2018a). Because fluid-rock reactions occur at low temperatures the newly formed minerals have O-isotope ratios significantly higher than the fluids they grow from ($1000\ln(\alpha_{r/w}) \sim 30$; Fig. S1), however, recrystallization is generally incomplete (i.e. the rocks are mixtures of fresh igneous phases and secondary minerals). Compiled whole-rock O-isotope compositions of seafloor lavas from modern ocean crust are heavier than fresh rocks (Fig. 2). They also have more variable O-isotope compositions than dikes and plutonic rocks, due to the more heterogeneous distribution of low-temperature alteration. Strikingly, lavas from Mesozoic age oceanic crust, altered when bottom water temperatures were relatively high (~15°C; e.g., Friedrich et al., 2012), commonly have substantially heavier O-isotope compositions than lavas altered under cooler bottom water conditions (≤5°C) in the late Cenozoic (Fig. 2). A Kolmogorov-Smirnov test of the difference in data distribution between the Mesozoic (arithmetic mean $\delta^{18}O_{SMOW}$ = 10.6‰; standard error = 0.3‰; geometric mean = 9.9‰; n = 210) and late Cenozoic samples (arithmetic mean $\delta^{18}O$ = 7.0‰; standard error = 0.1‰; geometric mean = 6.9‰; n = 151) confirms that the observed difference in $\delta^{18}O$ distribution is

statistically significant ($p = 10^{-22}$). The skewed distribution of the O-isotopic composition of >75 Myr old lavas is what would be expected if samples have been variably, and incompletely, replaced by a high $\delta^{18}O$ secondary mineral assemblage. This difference in the O-isotope composition of altered lavas (but not dikes or plutonics) as a function of their age cannot simply be a result of progressive ageing of the crust because most alteration in the lavas occurs in the first 20 Myrs after crustal accretion (e.g. Staudigel and Hart, 1985; Coogan and Gillis, 2018a). Nor can this be explained by the temperature dependence of $\alpha_{r/w}$, because cooler conditions lead to larger, not smaller, isotopic fractionations. Instead, the most likely explanation of the higher $\delta^{18}O$ of Mesozoic than late Cenozoic lavas is that they underwent greater extents of fluid-rock reaction and O-isotope exchange due to the higher bottom water temperature increasing reaction rates.

3. Sample suite and analytical techniques

To further investigate the controls on O-isotope exchange between seawater and lavas during off-axis hydrothermal circulation we have studied a ~20 km wide section of lavas exposed on the northern flank of the Cretaceous Troodos ophiolite (Supplementary Fig. S2). Whole-rock samples were collected along four traverses through the lava section (Coogan et al., 2017; Coogan and Gillis, 2018b). Carbonates were collected from throughout the study area and come mainly from amygdales but occasionally from vugs and veins. Whole-rock samples are variably altered to mineral assemblages that include clays, zeolites, calcite, K-feldspar, celadonite, chalcedony and Fe-oxy-hydroxides (e.g. Gillis and Robinson, 1990; Coogan and Gillis, 2018b).

Forty-six whole rock lavas were analysed for O-isotopes (Table S1) at Western University following procedures reported by Polat et al. (2018). Analyses of an in-house

quartz standard and a CO_2 gas standard gave $\delta^{18}O_{SMOW}$ = 11.44±0.27‰ (1 standard deviation; SD; n = 9) and 10.19±0.03‰ (1 SD; n = 11) relative to accepted values of 11.5‰ and 10.3‰. Three analyses of NBS28 (NIST RM 8546) run as an unknown gave $\delta^{18}O_{SMOW}$ = 9.61±0.02‰ (1 SD) relative to the accepted value of 9.58±0.09‰. The average standard deviation of replicate sample analyses was 0.39‰ (n = 12). The greater scatter in the sample than standard data suggests this reflects sample inhomogeneity. Strontium isotope ratios were also measured on samples not already analysed by Gillis et al. (2015) using identical procedures as in that study (Table S1).

Oxygen-isotope data for one hundred and eighty-four hand-picked carbonates from the study area are used to constrain the temperature of fluid-rock reaction (Table S2). Most were analysed at the University of British Columbia using a Delta PlusXL mass spectrometer in continuous flow mode as part of this project although some measurements come from previous studies and were performed in other laboratories (Gillis and Robinson, 1990; Gillis et al., 2015; all data are reported in Table S2). Duplicate analysis of the same powder gave results with an average absolute difference of 0.3‰. Complete sample duplication, including crushing and picking of different material from the same outcrop, led to a maximum difference of 1.4‰ (equivalent to ~7°C).

Eleven samples were selected for clumped-isotope analysis (Table S3) based on their spanning the normal range of $\delta^{18}O$ (i.e. excluding samples with extreme $\delta^{18}O$; see Section 4.1 and Fig. 4) and the geographical distribution of the study area (Fig. S2). The Sr and Mg contents of these samples were determined using standard ICP-MS (University of Victoria) and their $^{87}Sr/^{86}Sr$ by TIMS (University of British Columbia; Weis et al., 2006). Carbonate clumped-isotope thermometry is based on the quantification

of statistical anomalies in the abundance of doubly substituted isotopologues (e.g., $^{13}C^{18}O^{16}O^{16}O^{2-}$). For fundamental thermodynamic reasons, ^{13}C-^{18}O bonds in a carbonate mineral are more abundant in carbonates equilibrated at low than high temperatures (e.g. Schauble et al., 2006), and this distribution may be preserved over geologic time scales under favourable circumstances (Passey and Henkes, 2012; Stolper and Eiler, 2015). By precisely measuring the abundance of the multiply-substituted, mass-47, isotopologues in the CO_2 produced by acid digestion of a carbonate sample it is possible to constrain its original crystallization temperature without making assumptions regarding the composition of parent waters. Full analytical techniques are provided in Supplementary Material S1.

A concern for clumped isotope thermometry with samples as old as those studied here is that they may have undergone solid-state reordering. In this process the abundance of clumped carbonate groups in the mineral changes in response to the breaking and reformation of bonds within the mineral lattice (e.g. Passey and Henkes, 2012). As a thermally activated process solid-state reordering will reset T_c if the sample is held at sufficiently high temperature for sufficiently long. Experimental studies suggest that samples formed at near-surface temperatures, such as those studied here, must be heated to ≥100°C to induce measurable re-ordering on 100 Myr timescales (e.g. Passey and Henkes, 2012; Henkes et al., 2014; Stolper and Eiler, 2015). Based on the geological history of the study area (e.g. Robertson, 1977; Supplementary Material S3) we expected the carbonate clumped isotope distribution not to have been reset and, *a posteriori*, the low temperatures recorded by the clumped isotopes strongly support this.

4. Results

4.1. Calcite Δ_{47} and $\delta^{18}O$: aquifer fluid temperature and O-isotopic composition

The clumped isotope measurements yield average Δ_{47} ranging from 0.646 to 0.701‰. These data make it possible to estimate the temperature and oxygen-isotope composition of the water the calcite grew from provided we know the relationships between crystallization temperature (T_c) and Δ_{47} and between T_c and $\alpha_{c/w}$ (the $^{18}O/^{16}O$ fractionation factor between calcite and water). Precisely calibrating the clumped-isotope carbonate thermometer has long remained challenging, at least in part because of significant inter-laboratory discrepancies. For this reason, and following earlier studies from other groups, we interpret our results based on calibration data sets obtained in the same laboratory used to analyse the samples (Peral et al., 2018; Daëron et al., in review).

Theoretical models suggest that both the relationship between T_c and Δ_{47} (Watkins and Hunt, 2015) and between T_c and $\alpha_{c/w}$ (e.g. Watkins et al., 2013) may be influenced by kinetic factors. Recently Daëron et al. (in review) have reported that inorganic carbonates that grew very slowly, and which are likely to have formed in oxygen-isotope equilibrium with their parent waters, define a different T_c – Δ_{47} relationship than faster growing biogenic calcite. Additionally, they found further support for the suggestion that at typical laboratory growth rates (e.g. those of Kim and O'Neil, 1997) kinetic effects lead to non-equilibrium calcite $\delta^{18}O$ (e.g. Coplen, 2007; Watkins et al., 2013; Levitt et al., 2018). They interpret the very slow-growing inorganic carbonates as recording equilibrium compositions and suggest that the faster growing calcites have slightly higher Δ_{47} and substantially lower $\delta^{18}O$ due to kinetic isotope effects associated with higher calcification rates (Coplen, 2007; Watkins et al., 2013; Daëron et al., in review). Because calcite in the

upper oceanic crust forms over many millions of years (Staudigel and Hart, 1985; Coogan and Dosso, 2015), driven by the alkalinity generated by fluid-rock reactions, it seems likely that growth rates are generally slow in this setting. Thus, we initially use the slow-growth (equilibrium) calibrations reported by Daëron et al. (in review) to compute T_c from Δ_{47} and $\alpha_{c/w}$ from T_c (the latter being virtually identical to that of Coplen, 2007). This approach yields apparent crystallization temperatures between 13.8±2.1 and 29.0±2.4 °C (±1 standard error; Fig. 3a). Using these temperatures and the equilibrium (slow-growth) relationship between $\alpha_{c/w}$ and T_c (Coplen, 2007; Daëron et al., in review) allows the $\delta^{18}O$ of the fluid the calcite grew from to be determined. This results in a strongly bimodal distribution (Fig. 3b) of reconstructed water $\delta^{18}O_{VSMOW}$, with eight values tightly clustered around -1.0 ‰ (hereafter referred to as type A) and the remaining three around -3.5 ‰ (hereafter referred to as type B). Although different calibrations would lead to different absolute temperatures and fluid compositions, bimodality is an inherent feature of the data and would be present irrespective of the calibrations used.

In the Cretaceous, when the Troodos ophiolite formed, $\delta^{18}O_{SW}$ is thought to have been close to -1‰ due to the lack of ice sheets (e.g. Gregory and Taylor, 1981). Thus, the type A calcite can be explained as having grown slowly from a fluid with seawater-like $\delta^{18}O$. Such a model is consistent with the expectation that water-rock ratios are generally sufficiently high in off-axis hydrothermal systems that fluid-rock reactions are unlikely to substantially change the O-isotopic composition of the fluid. Clearly a different model is required to explain the type B calcites. Type B calcites are not obviously different to type A calcites in their C-isotopic composition, or Mg and Sr contents (Table S3). They also are from similar geological settings to the other samples (Fig. S2). The only independent

characteristics that differentiate the type B calcites are that they have the three highest $^{87}Sr/^{86}Sr$ ratios (Fig. 3, Fig. S4) and the three lowest Δ_{47}-derived temperatures (Fig. 3), which is unlikely to result from chance alone.

The Sr-isotopic composition of carbonates precipitated during alteration of the lava section of the oceanic crust depends both on the Sr-isotopic composition of seawater at the time the carbonate grew and the amount of basaltic Sr dissolved out of the rock into the fluid (e.g. Staudigel and Hart, 1985). The Sr-isotopic compositions of the type B carbonates are analytically indistinguishable from one another (0.707319-0.707322) but are higher than any of the other samples we measured clumped isotopes on (0.707280-0.707311). Based on comparison with the seawater Sr-isotope curve of McArthur and Howarth (2004), the type B calcite either formed at or before 91.7 Ma, or at or after 89.1 Ma (Fig. S4). The former age matches the age of the ophiolite raising the possibility that these three carbonates precipitated very soon after ophiolite formation from a fluid with $^{87}Sr/^{86}Sr$ almost identical to seawater. We consider two hypotheses to explain the type B calcite: (i) growth from an isotopically very light fluid; and (ii) disequilibrium (fast) growth.

According to the first hypothesis, the type B calcite grew from a fluid with $\delta^{18}O$ of roughly -3.5±0.3 ‰ which is substantially more ^{18}O depleted than the fluid the type A calcite are interpreted to have grown from and much lighter than Cretaceous seawater (Fig. 3). Fluid-rock reactions at low temperatures form minerals with high $\delta^{18}O$, leading to the lavas of the upper oceanic crust becoming isotopically heavy (Fig. 2), and hence the fluid in the lavas in the off-axis must be driven towards lower $\delta^{18}O$. Sufficient fluid-rock reaction, at a low water-to-rock ratio, could therefore lead to a fluid that was

isotopically much lighter than seawater. Indeed, this model has been proposed for upper-oceanic crust carbonates from ODP Site 801 that coupled Δ_{47} and $\delta^{18}O$ data suggest grew from an isotopically light fluid (Stolper et al., 2016). However, the lavas from ODP Site 801 have a complex geological history, including off-axis volcanism, that led to carbonate formation at anomalously high temperatures (up to >60°C; Alt and Teagle, 2003) that can only be maintained at low water-to-rock ratios. In contrast, both thermal and chemical constraints suggest that off-axis alteration normally occurs at high water-to-rock ratios (>1000; e.g. Coogan and Gillis, 2018a). Under these circumstances mass balance constraints mean that the bulk fluid cannot be driven to significantly lighter $\delta^{18}O$ than seawater.

Both thermal and chemical constraints require regional scale water-to-rock ratios in the lavas to be high. However, on a local scale the fluids could experience much smaller water-to-rock ratios. It is possible that this was the case for the fluid that the calcite in amygdales grew from because this fluid must have passed through a low-permeability rock to reach the vesicle. Is it possible that the fluid in vesicles had a much lower $\delta^{18}O$ than the bulk fluid in the lavas because of evolving in a local low-water-to-rock system? Three qualitative arguments suggest that this was not the case. First, all calcite $^{87}Sr/^{86}Sr$ are similar to that of late Cretaceous seawater indicating little modification of the fluid Sr-isotopic composition by rock dissolution (Fig. 3; Fig. S4). Since Sr-isotopes should be more strongly affected by rock dissolution than O-isotopes, little modification of the fluid O-isotopic composition is expected. Second, if fluid-rock reaction modified the fluid O-isotopic composition substantially then this should be seen most strongly in the calcite samples precipitated at higher temperatures because reaction

rates increase with increasing temperature. Instead, type B samples grew at the lowest temperatures based on their Δ_{47} (Fig. 3). Third, a continuum of calcite compositions would be expected in this scenario rather than the bimodal distribution we observed (Fig. 3). As a further test of whether fluid-rock reaction could have driven the fluid that the type B calcite grew from to low $\delta^{18}O$ we applied the model of DePaolo (2006) to calculate the expected difference between the composition of fluid in vesicles and in the main fluid flow channels in the lava section (Supplementary material S4). This modelling also suggests that the fluid from which the calcite grew had a similar $\delta^{18}O$ to the bulk fluid within the lavas. Because both empirical arguments and quantitative modelling suggest the fluid in the amygdales is unlikely to be substantially lighter than the main formation fluid we discount hypothesis (i).

The alternative hypothesis (ii) to explain the type B calcite is that these samples did not grow at equilibrium and hence the equilibrium relationships between T_c and Δ_{47}, and between T_c and $\alpha_{c/w}$, used to calculate the fluid $\delta^{18}O$ are inappropriate (Daëron et al., in review). This is most likely to be the case if the type B calcite grew faster than the other calcite (e.g. Devriendt et al., 2017; Levitt et al., 2018; Watkins et al., 2014; Watkins and Hunt, 2015), however we lack independent estimates of growth rates and so cannot directly test this model. To investigate this we reprocessed the type B raw data using relationships Δ_{47} and T_c, and between T_c and $\alpha_{c/w}$, appropriate for fast-growing calcite (from Peral et al. (2018) and Kim & O'Neil (1997) respectively). This increases the clumped-isotope temperatures for type B calcites by 3–4 °C, making them consistent with the lower range of type A temperatures, and brings the average predicted parental fluid $\delta^{18}O$ for type B calcites up to -1.4 ± 0.3 ‰ (1 SD). While potentially coincidental, the

observation that this model leads to the same fluid O-isotope ratio as that derived from the slow-growth model for the type A calcites, and the same as expected for Cretaceous seawater, leads us to explore this "growth rate control" model further.

Two ways in which the calcite growth rate may have varied substantially between samples are if the initial $CaCO_3$ phase was not calcite and this subsequently recrystallized to form calcite, or if the rate of calcite precipitation changed over time after crustal accretion. In the former model if, for example, the original $CaCO_3$ phase was aragonite and this subsequently transformed to calcite it is plausible this transformation occurred rapidly leading to disequilibrium calcite growth. We have no reason to believe that recrystallization of a precursor phase occurred and consider this a somewhat ad hoc, although plausible, explanation of the type B calcite. Our favoured model is that a change in calcite precipitation rate over time occurred. One might expect a change in the rate of calcite formation over time after crustal accretion because the reactions that drive calcite formation will be fastest when the crust is youngest and hence least altered. There are multiple possible causes of an age dependence of rock dissolution rates such as evolution of mineral surface roughness, accumulation of leached layers and secondary precipitates and decreases in the reaction affinity driving dissolution (e.g. White and Brantley, 2003). Furthermore, observational support for a change in calcite formation rate with time after crustal accretion comes from model ages of calcite in the oceanic crust (Coogan and Dosso, 2015). If the type B calcite grew when the crust was young, and hence most reactive, the rate of alkalinity generation (and hence calcite precipitation) would have been the highest and hence calcite formation rates would also have been the highest. It is plausible that at this stage growth rates were sufficiently rapid so as to lead to

disequilibrium calcite compositions. This model is consistent with the observation that the Sr-isotope ratios of the type B calcite match that of seawater at the time of ophiolite formation, but the type A calcite have lower $^{87}Sr/^{86}Sr$ (Fig. 3; Fig. S4).

In summary, eight out of eleven carbonates (type A) measured for clumped isotopes are most simply interpreted as having grown slowly in O-isotope (and clumped-isotope) equilibrium with a fluid with $\delta^{18}O$ of -0.94±0.30‰ (1 SD) at between 18.6±2.2 and 29.0±2.4°C (Fig. 3). The other three samples (type B) could be explained by faster (disequilibrium) growth from a fluid with a similar O-isotope composition, with kinetic isotope effects leading to the different calcite compositions. Disequilibrium growth could occur during the initial stages of alteration of the lavas when the rocks are most reactive (e.g. contains copious, unarmored, glass) and hence the rate of calcite formation the highest.

If we assume that all of the carbonates grew from a fluid with $\delta^{18}O$ of approximately -1‰ then we can use standard O-isotope thermometry to determine the precipitation temperatures of all of the carbonates analysed for $\delta^{18}O$. The majority of the samples give temperatures of 20±6°C (1 SD) using the Daëron et al. (in review), or, equivalently, the Coplen (2007) relationship (Fig. 4). Bottom water temperature in the first 20 Myr after accretion of the Troodos crust, when most calcite forms (Coogan and Gillis, 2018a), was ~15±7°C (Friedrich et al., 2012). Thus, the vast majority of calcite was precipitated at only ~5°C above bottom water temperature. If the Kim and O'Neil (1997) thermometer was used instead the calculated temperatures decrease by 7 to 10°C and ~15% of the samples have calculated precipitation temperatures <8°C, which is lower than bottom water temperatures.

4.2. Silicate $\delta^{18}O$: extent of rock recrystallization

Figure 2 shows that the bulk-rock $\delta^{18}O$ of lavas from Cretaceous age oceanic crust is higher than that for late Cenozoic crust. Since $\delta^{18}O_{SW}$ was lower in the Cretaceous than late Cenozoic (due to the lack of ice sheets) this suggests that the extent of O-isotope exchange was greater in the Cretaceous. Because the temperature of fluid-rock reaction in the lavas is only slightly above that of bottom water (Fig. 3, 4) it seems likely that the higher bottom water temperature in the Cretaceous led to greater extents of O-isotope exchange between the lavas and ocean at that time than in the late Cenozoic. To further investigate O-isotope exchange between the lavas and ocean we collected data for whole-rock samples from the Troodos lavas that have also been analysed for their major element and Sr-isotopic compositions.

Whole-rock $\delta^{18}O$ generally decreases with depth in the lava pile in each of the four lava sections in the Troodos ophiolite studied here, from a maximum of ~26‰ down to a minimum of ~8‰ (Fig. 5a) compared to a fresh rock $\delta^{18}O$ of ~ 5.8±0.5‰ (Supplementary Material S3). The extent of enrichment in ^{18}O in the altered lavas correlates with the enrichment in K_2O (Fig. 5d) and depletion in both Na_2O (Fig. 5c) and CaO from the silicate portion of the rock (CaO_{sil}; Fig. 5b). Almost all of the silicate-hosted Ca in the original rock has been leached from the samples with the highest whole-rock $\delta^{18}O$. Whole-rock $\delta^{18}O$ and $^{87}Sr/^{86}Sr_{(i)}$ (the age corrected initial Sr-isotopic ratio) also correlate strongly (Fig. 5e). Samples with the highest $\delta^{18}O$ have $^{87}Sr/^{86}Sr_{(i)}$ similar to late Cretaceous seawater; i.e. these samples completely equilibrated their Sr-isotopic composition with seawater during low-temperature alteration. Overall these observations point to the extent of O-isotope enrichment being largely controlled by the extent of

recrystallization of the primary rock with complete recrystallization leading to a bulk-rock $\delta^{18}O$ of ~26‰.

Most samples from the modern ocean basins that have been analysed for O-isotopes have not also been analysed for major elements and Sr-isotopes preventing us from determining whether the correlations observed in the Troodos samples are a general feature of all altered lavas. Two locations from which samples have been more systematically analysed are the adjacent DSDP Holes 417A, 417D and 418A (120 Myr old Atlantic crust) and ODP Hole 801C (156 Myr old Pacific crust). For these cores so-called composite samples have been analysed more extensively than individual samples generally are. Similar correlations of whole-rock O-isotopic composition and K_2O, Na_2O and CaO_{sil} contents and $^{87}Sr/^{86}Sr_{(i)}$ are observed in the composite samples from DSDP Sites 417A, 417D and 418A and, for K_2O and Na_2O, in Hole 801C (data are not available for the other species for this core) suggesting that these are general characteristics of altered upper oceanic crust (Fig. 5).

Major element exchange between the ocean and oceanic crust during low-temperature hydrothermal circulation acts as a source of alkalinity to the fluid or, in other words, as a sink of CO_2 from the ocean-atmosphere system (Spivack and Staudigel, 1994; Coogan and Gillis, 2013). The magnitude of the alkalinity source can be determined by charge balance between the bulk composition of an altered rock and an estimate of its protolith composition (e.g. Spivack and Staudigel, 1994). The alkalinity produced by each sample increases roughly linearly with the O-isotopic composition of the sample (Fig. 5f). Thus, greater extents of fluid-rock reaction in the upper oceanic crust lead to both greater extents of O-isotope exchange and greater CO_2 consumption. The extent of

CO_2 consumption has previously been shown to correlate with bottom water temperature (Gillis and Coogan, 2011) and the greater extent of O-isotope exchange in Cretaceous lavas than late Cenozoic lavas (Fig. 2) suggests that this is also dependent on bottom water temperature.

Additional evidence for alteration of the lavas at low-temperatures is provided by three celadonite separates collected from void spaces in the lava pile in the Troodos ophiolite that have $\delta^{18}O$ of 21±1‰ (Table 1). The consistency of their O-isotopic composition suggests precipitation from a fluid with a similar temperature and O-isotopic composition. Using the isotopic fractionation factor for glauconite (Fig. S2) and a fluid $\delta^{18}O$ of -1‰ this would reflect equilibrium at ~16°C. While the fractionation factor is not well enough known to have confidence in the exact temperature, it seems likely that the celadonites grew at temperatures little above that of bottom water consistent with constraints from calcite thermometry (Fig. 3; Fig. 4).

5. Discussion: the CO_2-cycle as a buffer on seawater $\delta^{18}O$

The data presented above suggest that: (i) off-axis hydrothermal alteration of the upper oceanic crust typically occurs at only ~5°C above bottom water temperature, with the fluid O-isotopic composition remaining close to that of seawater (Fig. 3; Fig. 4); (ii) the extent of alteration and O-isotope exchange between the ocean and lavas depends on bottom water temperature (Fig. 2; Gillis and Coogan, 2011; Coogan and Gillis, 2018b); and (iii) the extent of O-isotope exchange and alkalinity generation are linked (Fig. 5f). Here we use these observations to constrain a model of the O-isotope evolution of seawater.

The model of the O-isotope composition of seawater considers O-isotope fluxes associated with on- and off-axis hydrothermal alteration of the oceanic crust, continental chemical weathering, and the precipitation of sedimentary carbonates from the ocean (Table 1; Fig. S5). Each flux depends on the mass of material involved in the flux and the changes in O-isotopic composition between the protolith and final rock (Table 1; Eq. S1). For seafloor weathering and continental weathering the mass fluxes depend on global mean temperature such that higher temperatures lead to higher weathering fluxes. Surface temperature is set such that the prescribed CO_2 degassing flux is balanced by the CO_2 consumption via these two weathering fluxes; i.e. the O-isotope model is linked to the stabilizing feedbacks of the long-term C-cycle. Such a link has also been recently suggested by Ryb and Eiler (2018). The fractionation of O-isotopes during high-temperature alteration of dikes and plutonic rocks at mid-ocean ridges is calculated based on the compiled data (Fig. 2). The fractionation of O-isotopes during seafloor weathering, continental weathering and carbonate sedimentation are dependent on global temperature. The solid earth CO_2 degassing flux can either be coupled with, or decoupled from, the rate of oceanic crustal formation. The values of many model parameters are not known precisely and so we use Monte Carlo simulations to explore how $\delta^{18}O_{SW}$ varies as a function of the controlling parameters.

The model results suggest that, irrespective of the uncertainty in the input parameters, the $\delta^{18}O$ of seawater should remain close to the modern value if the rate of solid earth degassing is closely tied to the rate of oceanic crust creation (Fig. 6a). In this scenario, increased CO_2 degassing leads (through increased surface temperature) to an increased weathering rate on both the seafloor and continents and increased carbonate

sediment formation. In turn, because these processes operate at low temperatures, this increases the removal rate of ^{18}O from the ocean. However, this increased sink for ^{18}O is counterbalanced by the larger mass of dikes and plutonic rocks reacting with seawater on-axis at high-temperatures which increases the flux of ^{18}O into the ocean. This result is relatively insensitive to the activation energy for both seafloor and continental weathering. The dominant control on the scatter in model $\delta^{18}O_{SW}$ is the thickness of the sheeted dike complex (and to a lesser extent the plutonic complex) with models with thicker sheeted dike complexes having a larger flux of ^{18}O into the ocean from the dikes, and hence higher $\delta^{18}O_{SW}$. In the modern oceans the thickness of the sheeted dike complex depends on the depth of the magma reservoir feeding lava flows and is principally controlled by spreading rate. Global average spreading rates may have fluctuated over the Phanerozoic but are unlikely to have changed systematically. Further back in Earth history, if higher mantle heat loss was dissipated through faster spreading, average sheeted dike complexes may have been thinner perhaps reducing the flux of ^{18}O into the ocean.

It is possible that solid Earth CO_2 degassing has been decoupled from the rate of formation of new seafloor either during geologically brief periods (e.g. during formation of large igneous provinces) or if Earth's tectonic regime was substantially different in the past. In this scenario, all other things being equal, increased CO_2 degassing leads to an increase in the mass of low-temperature mineral formation required to balance the alkalinity budget of the ocean, and hence an increased sink for ^{18}O (whether in the upper oceanic crust or on the continents). This leads to a decrease in $\delta^{18}O_{SW}$ with increasing CO_2 degassing (Fig. 6b).

Over long periods of time models that closely link solid earth degassing rate and oceanic crustal production rate are probably more realistic than those that do not (e.g. Berner, 1991). Additionally, irrespective of whether the rates of solid earth CO_2 degassing and oceanic crust formation are linked, limited systematic variation in either parameter is expected over the Phanerozoic. This is because both are expected to be generally related to the secular cooling of the mantle, which has been limited over this time. Thus, it seems unlikely that the isotopic composition of seawater has increased systematically over the Phanerozoic by ~6‰ as has been suggested. Alternative models to explain the carbonate and chert $\delta^{18}O$ data for early Phanerozoic samples will probably have to be found. This conclusion is consistent with recent work using clumped isotope analysis of Phanerozoic carbonates (e.g. Came et al., 2007; Cummins et al., 2014; Finnegan et al., 2011; Henkes et al., 2018; Ryb and Eiler, 2018) that suggest that $\delta^{18}O_{SW}$ has not changed substantially over the Phanerozoic.

Our model reveals a problem in a currently popular hypothesis to explain the purported increase in $\delta^{18}O_{SW}$ over the Phanerozoic, that proposes that increased pelagic sedimentation reduced ingress of seawater into the upper oceanic crust, thus decreasing the extent of seafloor weathering over this time (Wallmann, 2004, Kasting et al., 2006; Jaffrés et al., 2007). This model does not account for the alkalinity balance. All other things being equal, decreased seafloor weathering would require increased continental weathering to balance the C-cycle. In turn, the removal of ^{18}O from the ocean would simply shift from the upper oceanic crust to continental margin sediments; this ^{18}O sink would not disappear as would be required to drive a large increase in $\delta^{18}O_{SW}$ over the Phanerozoic.

The suggestion that the O-isotopic composition of seawater is unlikely to have changed much over the Phanerozoic is not new (e.g. Muehlenbachs and Clayton, 1976; Gregory and Taylor, 1981; Muehlenbachs, 1998) but our explanation for why this is the case differs significantly from most previous work. Previous models have commonly suggested that alteration of the oceanic crust buffers the O-isotopic composition of the ocean based on fixed extents of high- and low-temperature alteration driving the ocean to be ~6‰ lighter than the oceanic crust. Instead, we suggest that because many of the same processes control both the O-isotopic composition of seawater and the long-term carbon cycle, the feedbacks related to the latter prevent the O-isotopic composition of seawater changing dramatically, at least over the Phanerozoic.

5.1. Unravelling the history of $\delta^{18}O_{SW}$

Because clumped isotope analysis of seafloor carbonates from ophiolites appears to allow the O-isotopic composition of the deep ocean to be determined from ophiolite samples (Fig. 3), analysis of ophiolite-hosted carbonate may provide a mechanism to determine the long-term history of the O-isotopic composition of the deep ocean. This would avoid some of the uncertainties associated with similar studies using shallow marine carbonates (e.g., Came et al., 2007; Cummins et al., 2014; Finnegan et al., 2011; Henkes et al., 2018) where the water the carbonate precipitated from may not be representative of the average global ocean (e.g. Muehlenbachs, 1998). However, we caution that the low-temperature seafloor weathering of the lava section of the Troodos ophiolite is exceptionally preserved, and the samples studied here come from the best studied part of this ophiolite. Even with this context we see complexity in interpreting the data due to the apparent growth-rate control on the composition of some samples (Fig. 3).

Using similar approaches on older, and less well-preserved, ophiolites will require very careful consideration of whether the material studied really preserves a record of the growth conditions.

6. Conclusions

Using both new and compiled isotope data for whole-rock samples and carbonates from the lava section of the oceanic crust we: (i) have confirmed that alteration of the lavas typically occurs at near bottom water temperature with the fluid flux being sufficient that only minor changes in the O-isotopic composition of the formation fluid generally occur; (ii) show that the extent of O-isotopic exchange between seafloor lavas and seawater correlates with the extent of exchange of other components including alkalinity generation and is greater when bottom water temperature is higher (Fig. 2; Fig. 5); and (iii) introduce a simple model for the O-isotopic evolution of seawater that links the O-isotope and C-cycles. In this model the O-isotopic composition of seawater cannot change substantially over time if the rate of CO_2 degassing from the solid earth is tied to the rate of spreading at mid-ocean ridges. This is because while increased oceanic crustal production leads to an increased flux of ^{18}O to the oceans through high-temperature alteration of dikes and plutonic rocks at mid-ocean ridges, this is counter balanced by an increased CO_2 flux requiring increased low-temperature weathering (of seafloor lavas and/or the continents) which provides an increased ^{18}O sink. A roughly invariant $\delta^{18}O_{SW}$ is thus an expected consequence of the required balance between CO_2 degassing and drawdown.

Acknowledgments

Two anonymous reviewers and editor Louis Derry are thanked for their comments which improved the manuscript. The Geological Survey of Cyprus is thanked for access to the field area and their ongoing interest in our work. Fred Longstaffe is thanked for the whole-rock O-isotope data, Janet Gabites for standard carbonate O-isotope analyses, and John McAuthur for providing his seawater Sr-isotope curve. Aerona Moore, Matt Pope, Michaella Yakimoski, Margo Ramsay, Hunter Markvoort and Sebastian Bichlmaier are thanked for help in picking the carbonates used in this study. The analytical facilities at LSCE benefitted from financial support from: Région Ile-de-France; Direction des Sciences de la Matière du Commissariat à l'Energie Atomique; Institut National des Sciences de l'Univers, Centre National de la Recherche Scientifique; Universtité de Versailles/Saint-Quentin-en-Yvelines; and Plateforme Analytique Géosciences Paris Saclay (PANOPLY). LAC and KMG were funded through NSERC Discovery (5098 & 155396) and Accelerator grants. The manuscript was largely prepared while the authors were guests at the Institute of Marine Sciences in Barcelona.

References

Alt, J.C., 2003. Stable isotopic composition of upper oceanic crust formed at a fast spreading ridge, ODP Site 801. Geochemistry, Geophys. Geosystems 4, doi:10.1029/2002GC000400.

Alt, J.C., Muehlenbachs, K., Honnorez, J., 1986. An oxygen isotopic profile through the upper kilometer of the oceanic crust, DSDP Hole 504B. Earth Planet. Sci. Lett. 80, 217–229.

Alt, J.C., Teagle, D.A.H., 2003. Hydrothermal alteration of upper oceanic crust formed at a fast-spreading ridge: mineral, chemical, and isotopic evidence from ODP Site 801. Chem. Geol. 201, 191–211.

Came, R.E., Eiler, J.M., Veizer, J., Azmy, K., Brand, U., Weidman, C.R., 2007. Coupling of surface temperatures and atmospheric CO_2 concentrations during the Palaeozoic era. Nature 449, 198-201.

Coogan, L.A., Gillis, K.M., Pope, M., Spence, J., 2017. The role of low-temperature (off-axis) alteration of the oceanic crust in the global Li-cycle: Insights from the Troodos ophiolite. Geochim. Cosmochim. Acta 203, 201–215.

Coogan, L.A., Dosso, S.E., 2015. Alteration of ocean crust provides a strong temperature dependent feedback on the geological carbon cycle and is a primary driver of the Sr-isotopic composition of seawater. Earth Planet. Sci. Lett. 415, 38–46.

Coogan, L.A., Gillis, K.M., 2018a. Low-Temperature Alteration of the Seafloor: Impacts on Ocean Chemistry. Annu. Rev. Earth Planet. Sci. 46, 21-45.

Coogan, L.A., Gillis, K.M., 2018b. Temperature dependence of chemical exchange during seafloor weathering: Insights from the Troodos ophiolite. Geochim. Cosmochim. Acta 243, 24–41.

Coplen, T.B., 2007. Calibration of the calcite-water oxygen isotope thermometer at Devils Hole, Nevada, a natural laboratory. Geochim. Cosmochim. Acta 71, 3948–3957.

Cummins, R.C., Finnegan, S., Fike, D.A., Eiler, J.M., Fischer, W.W., 2014. Carbonate clumped isotope constraints on Silurian ocean temperature and seawater $\delta^{18}O$. Geochim. Cosmochim. Acta 140, 241–258.

Daëron, M., Drysdale, R.N., Peral, M., Huyghe, D., Blamart, D., Coplen, T.B., Lartaud, F., Zanchetta, G. (in review) Most Earth-surface calcites precipitate out of isotopic equilibrium, Nature communications.

DePaolo, D.J., 2006. Isotopic effects in fracture-dominated reactive fluid-rock systems. Geochim. Cosmochim. Acta 70, 1077–1096.

Devriendt, L.S., Watkins, J.M., McGregor, H. V, 2017. Oxygen isotope fractionation in the $CaCO_3$-DIC-H_2O system. Geochim. Cosmochim. Acta 214, 115–142.

Finnegan, S., Bergmann, K., Eiler, J.M., Jones, D.S., Fike, D.A., Eisenman, I., Hughes, N.C., Tripati, A.K., Fischer, W.W., 2011. The Magnitude and Duration of Late Ordovician/Early Silurian Glaciation. Science 331, 903–906.

Friedrich, O., Norris, R.D., Erbacher, J., 2012. Evolution of middle to Late Cretaceous oceans—A 55 m.y. record of Earth's temperature and carbon cycle. Geol. 40, 107–110.

Fritz, P., 1971. Geochemical characteristics of dolomites and the ^{18}O content of Middle Devonian oceans. Earth Planet. Sci. Lett. 11, 277–282.

Gillis, K.M., Coogan, L.A., 2011. Secular variation in carbon uptake into the ocean crust. Earth Planet. Sci. Lett. 302, 385–392.

Gillis, K.M., Coogan, L.A., Brant, C., 2015. The role of sedimentation history and lithology on fluid flow and reactions in off-axis hydrothermal systems: A perspective from the Troodos ophiolite. Chem. Geol. 414, 84–94.

Gillis, K.M., Robinson, P.T., 1990. Patterns and processes of alteration in the lavas and dykes of the Troodos Ophiolite, Cyprus. J. Geophys. Res. 95, 21,521-21,548.

Gregory, R.T., Taylor, H.P., 1981. An oxygen isotope profile in a section of Cretaceous oceanic crust, Samail Ophiolite, Oman: Evidence for $\delta^{18}O$ buffering of the oceans by deep (>5 km) seawater-hydrothermal circulation at mid-ocean ridges. J. Geophys. Res. Solid Earth 86, 2737–2755.

Henkes, G.A., Passey, B.H., Grossman, E.L., Shenton, B.J., Pérez-Huerta, A., Yancey, T.E., 2014. Temperature limits for preservation of primary calcite clumped isotope paleotemperatures. Geochim. Cosmochim. Acta 139, 362–382.

Henkes, G.A., Passey, B.H., Grossman, E.L., Shenton, B.J., Yancey, T.E., Pérez-Huerta, A., 2018. Temperature evolution and the oxygen isotope composition of Phanerozoic oceans from carbonate clumped isotope thermometry. Earth Planet. Sci. Lett. 490, 40–50.

Jaffrés, J.B.D., Shields, G.A., Wallmann, K., 2007. The oxygen isotope evolution of seawater: A critical review of a long-standing controversy and an improved geological water cycle model for the past 3.4 billion years. Earth-Science Rev. 83, 83–122.

Kasting, J.F., Howard, M.T., Wallmann, K., Veizer, J., Shields, G., Jaffrés, J., 2006. Paleoclimates, ocean depth, and the oxygen isotopic composition of seawater. Earth Planet. Sci. Lett. 252, 82–93.

Kelley, K.A., Plank, T., Ludden, J.N., Staudigel, H., 2003. Composition of altered oceanic crust at ODP Sites 801 and 1149. Geochemistry Geophys. Geosystems 4, doi:10.1029/2002GC000435.

Kim, S.-T., O'Neil, J.R., 1997. Equilibrium and non-equilibrium oxygen isotope effects in synthetic carbonates. Geochim. Cosmochim. Acta 61, 3461–3475.

Kirchner, T.M., Gillis, K.M., 2012. Mineralogical and strontium isotopic record of hydrothermal processes in the lower ocean crust at and near the East Pacific Rise. Contrib. Mineral. Petrol. 164, 123–141.

Lécuyer, C., Allemand, P., 1999. Modelling of the oxygen isotope evolution of seawater: implications for the climate interpretation of the $\delta^{18}O$ of marine sediments. Geochim. Cosmochim. Acta 63, 351–361.

Levitt, N.P., Eiler, J.M., Romanek, C.S., Beard, B.L., Xu, H., Johnson, C.M., 2018. Near Equilibrium ^{13}C-^{18}O Bonding During Inorganic Calcite Precipitation Under Chemo-Stat Conditions. Geochemistry, Geophys. Geosystems, 19, 901–920. https://doi.org/10.1002/2017GC007089.

McArthur, J. M., & Howarth, R. J. (2004). Strontium Isotope Stratigraphy. In F. M. Gradstein, J. G. Ogg, & A. G. Smith (Eds.), A Geological Time Scale (pp. 96–105). Cambridge: Cambridge University Press.

Muehlenbachs, K., 1998. The oxygen isotopic compostion of the oceans, sediment and the seafloor. Chem. Geol. 145, 263–273.

Muehlenbachs, K., Clayton, R.N., 1976. Oxygen isotope composition of the oceanic crust and its bearing on seawater. J. Geophys. Res. 81, 4365–4369.

Passey, B.H., Henkes, G.A., 2012. Carbonate clumped isotope bond reordering and geospeedometry. Earth Planet. Sci. Lett. 351–352, 223–236.

Peral, M., Daëron, M., Blamart, D., Bassinot F., Dewilde, F., Smialkowskii, N., Isguder, G., Bonnin, J., Jorissen, F., Kissel, C., Michel, E., Riveiros, N.V., Waelbroeck, C., 2018. Updated calibration of the clumped isotope thermometer in planktonic and benthic foraminifera, Geochimica et Cosmochimica Acta, 239, 1-16.

Perry, E.C., 1967. The oxygen isotope chemistry of ancient cherts. Earth Planet. Sci. Lett. 3, 62–66.

Robertson, A.H.F., 1977. Tertiary uplift history of the Troodos massif, Cyprus. GSA Bull. 88, 1763–1772.

Ryb, U., Eiler, J.M., 2018. Oxygen isotope composition of the Phanerozoic ocean and a possible solution to the dolomite problem. Proc. Natl. Acad. Sci., http://www.pnas.org/content/early/2018/06/06/1719681115.

Savin, S.M., Epstein, S., 1970. The oyxgen and hydrogen isotope geochemistry of ocean sediments and shales. Geochim. Cosmochim. Acta 34, 43–63.

Schauble, E.A., Ghosh, P., Eiler, J.M., 2006. Preferential formation of 13C–18O bonds in carbonate minerals, estimated using first-principles lattice dynamics. Geochim. Cosmochim. Acta 70, 2510–2529.

Shields, G., Veizer, J., 2002. Precambrian marine carbonate isotope database: Version 1.1. Geochemistry, Geophys. Geosystems 3, 1-12.

Spivack, A.J., Staudigel, H., 1994. Low-temperature alteration of the upper oceanic crust and the alkalinity budget of seawater. Chem. Geol. 115, 239–247.

Staudigel, H., Hart, S.R., 1985. Dating of ocean crust hydrothermal alterantion: Strontium isotope ratios from Hole 504B carbonates and reinterpretation of Sr Isotope data from Deep Sea Drilling Project Sites 105, 332, 417, and 418. Init. Rep. Deep Sea Drill. Proj. 83, 297–303.

Staudigel, H., Plank, T., White, B., Schimincke, H.-U., 1996. Geochemical fluxes during seafloor alteration of the basaltic upper oceanic crust: DSDP Sites 417 and 418, in:

Subduction: Top to Bottom. American Geophysical Union, Washington, DC, pp. 19–38.

Stolper, A. D., Eiler, J. M., 2015. The kinetics of solid-state isotope-exchange reactions for clumped isotopes: A study of inorganic calcites and apatites from natural and experimental samples. Am. J. Sci. 315, 363–411.

Stolper, A, D., Antonelli, M. A, Ramos, D.S., Bender, M. L Schrag, D.P., DePaolo, D.J., Higgins, J.A., 2016. Isotopic constraints on the formation of carbonates during low-temperature hydrothermal oceanic crust alteration, in: American Geophysical Union, Fall General Assembly 2016, Abstract Id. PP22B-04.

Turchyn, A. V, Alt, J.C., Brown, S.T., DePaolo, D.J., Coggon, R.M., Chi, G., Bédard, J.H., Skulski, T., 2013. Reconstructing the oxygen isotope composition of late Cambrian and Cretaceous hydrothermal vent fluid. Geochim. Cosmochim. Acta 123, 440–458.

Veizer, J., Ala, D., Azmy, K., Bruckenschen, P., Buhl, D., Bruhn, F., Carden, G.A.F., Diener, A., Ebneth, S., Godderis, Y., Jasper, T., Korte, C., Pawellek, F., Podlaha, O.G., Strauss, H., 1999. $^{87}Sr/^{86}Sr$, $\delta^{13}C$ and $\delta^{18}O$ evolution of Phanerozoic seawater. Chem. Geol. 161, 59–88.

Veizer, J., Prokoph, A., 2015. Temperatures and oxygen isotopic composition of Phanerozoic oceans. Earth-Science Rev. 146, 92–104.

Walker, J.C.G., Lohmann, K.C., 1989, Why the oxygen isotopic composition of seawater changes with time. Geophys. Res. Lett. 16, 323–326.

Wallmann, K., 2004. Impact of atmospheric CO_2 and galactic cosmic radiation on Phanerozoic climate change and the marine delta O-18 record. Geochemistry Geophys. Geosystems 5, doi:10.1029/2003GC000683.

Watkins, J.M., Hunt, J.D., 2015. A process-based model for non-equilibrium clumped isotope effects in carbonates. Earth Planet. Sci. Lett. 432, 152–165.

Watkins, J.M., Hunt, J.D., Ryerson, F.J., DePaolo, D.J., 2014. The influence of temperature, pH, and growth rate on the $\delta^{18}O$ composition of inorganically precipitated calcite. Earth Planet. Sci. Lett. 404, 332–343.

Watkins, J.M., Nielsen, L.C., Ryerson, F.J., DePaolo, D.J., 2013. The influence of kinetics on the oxygen isotope composition of calcium carbonate. Earth Planet. Sci. Lett. 375, 349–360.

White, A.F., Brantley, S.L., 2003. The effect of time on the weathering of silicate minerals: why do weathering rates differ in the laboratory and field? Chem. Geol. 202, 479–506.

Figures

Figure 1. Schematic illustration (not to scale) of the processes in the oceanic crust that modify $\delta^{18}O_{SW}$. Reactions associated with on-axis hydrothermal circulation mainly occur in the sheeted dikes, where fluid flow is driven by the cooling of magma chambers (red ellipse in figure) and plutonic rocks with lesser fluid flow through the plutonics. For the modern system ($\delta^{18}O_{SW}$ ~0‰) these high-temperature reactions lead to the rocks becoming isotopically lighter relative to the fresh rocks (5.7‰). Off-axis hydrothermal circulation in the lava section of the crust, that occurs across the abyssal plains at low-temperatures, leads to the rocks becoming isotopically heavier. Fluid flow is shown as arrows; black = cool; yellow = hot; dashing indicates smaller, but less well known, fluid fluxes (in the plutonic section).

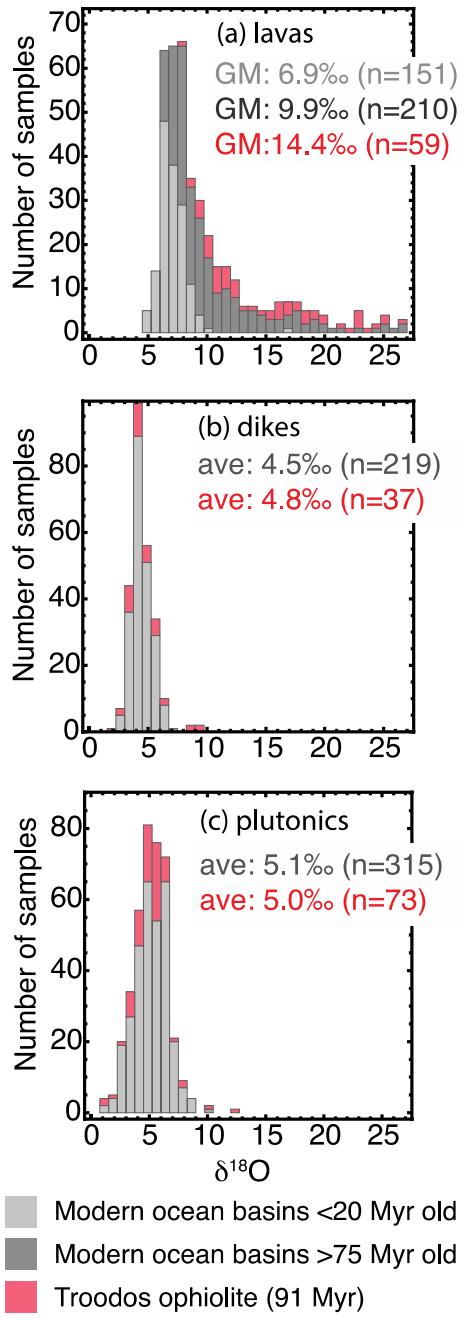

Figure 2: Histograms of compiled and new (see later) O-isotope compositions of lavas (VSMOW), dikes and plutonic rocks from the modern ocean basins and the Troodos ophiolite. The data for dikes and plutonic rocks from the modern ocean basins are all

from <20 Myr old crust and have very similar distributions to the same lithologies in the Cretaceous Troodos ophiolite. In contrast, there is a distinct difference between lava samples from young (<20 Myr) and old (>75 Myr) crust with the Troodos ophiolite samples being more similar to the older samples from the modern ocean basins. Because of the non-normal data distribution for lavas geometric means (GM) are given instead of arithmetic means (ave). Sources of data are listed in Supplementary Table S4.

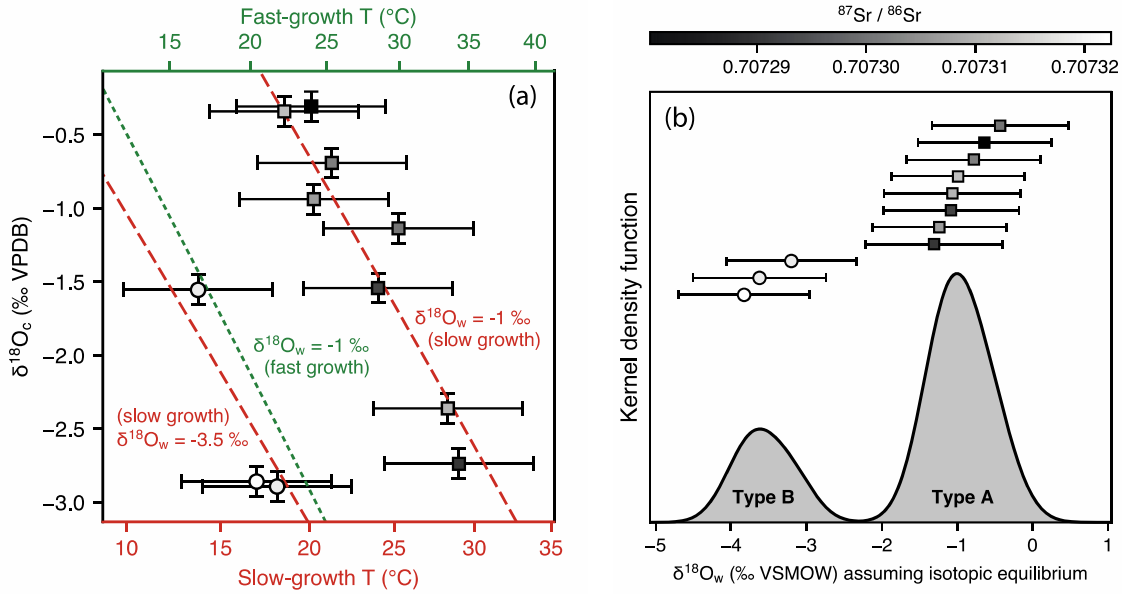

Figure 3. (a) Δ_{47}-derived carbonate precipitation temperature plotted against carbonate $\delta^{18}O$, with 95% confidence limits. Eight of the eleven samples lie on the trend predicted for slow (equilibrium; red lines) growth from a water (subscript W) with $\delta^{18}O$ of -1‰ (as expected for Cretaceous seawater). The other three samples can be explained either as having grown from a fluid that was ~3‰ lighter or as having grown fast (green line), with kinetic isotope fractionation, from a fluid with $\delta^{18}O$ of -1‰; see text for discussion; (b) kernel density plots showing that the fluid O-isotope compositions calculated assuming equilibrium relationships (see text for discussion) fall into two distinct groups (type A and type B) that also have different, although similar, Sr-isotopic compositions (as shown by the symbol grey-scale in both part a and b).

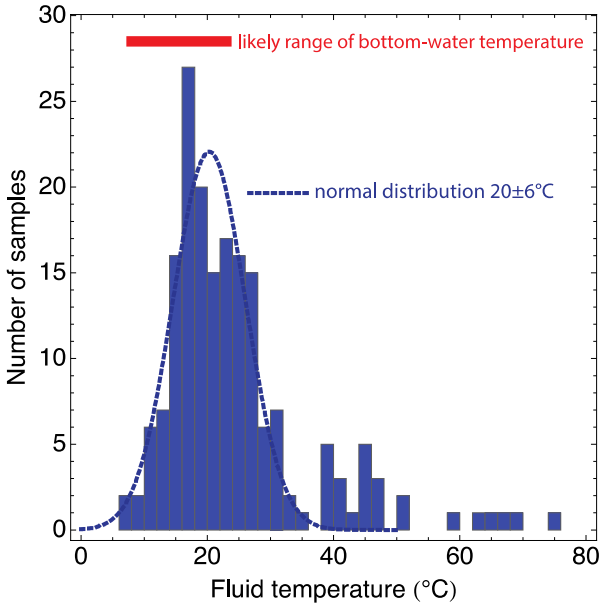

Figure 4. Histogram of the calculated temperature of carbonate precipitation based on standard $\delta^{18}O$ thermometry for samples from the Troodos lavas (n = 184) assuming a fluid $\delta^{18}O$ of -1‰ using the Daëron et al. (in review) calibration (which is virtually identical to the Coplen (2007) thermometer). The blue curve shows the probability distribution for the average (20.3°C) and standard deviation (5.8°C) of all carbonate-derived temperatures <38°C, which captures the distribution of the coolest 86% of the data. Higher temperatures are generally associated with deeper levels in the lavas, where the amount of carbonate is dramatically lower than at shallower crustal levels and fluid fluxes smaller, as well as in isolated regions interpreted as up-flow zones. The red bar shows the range in bottom water temperature during the first 20 Myrs after formation of the ophiolite (Friedrich et al., 2012), which is the main time interval of carbonate formation (e.g. Coogan and Gillis, 2018a).

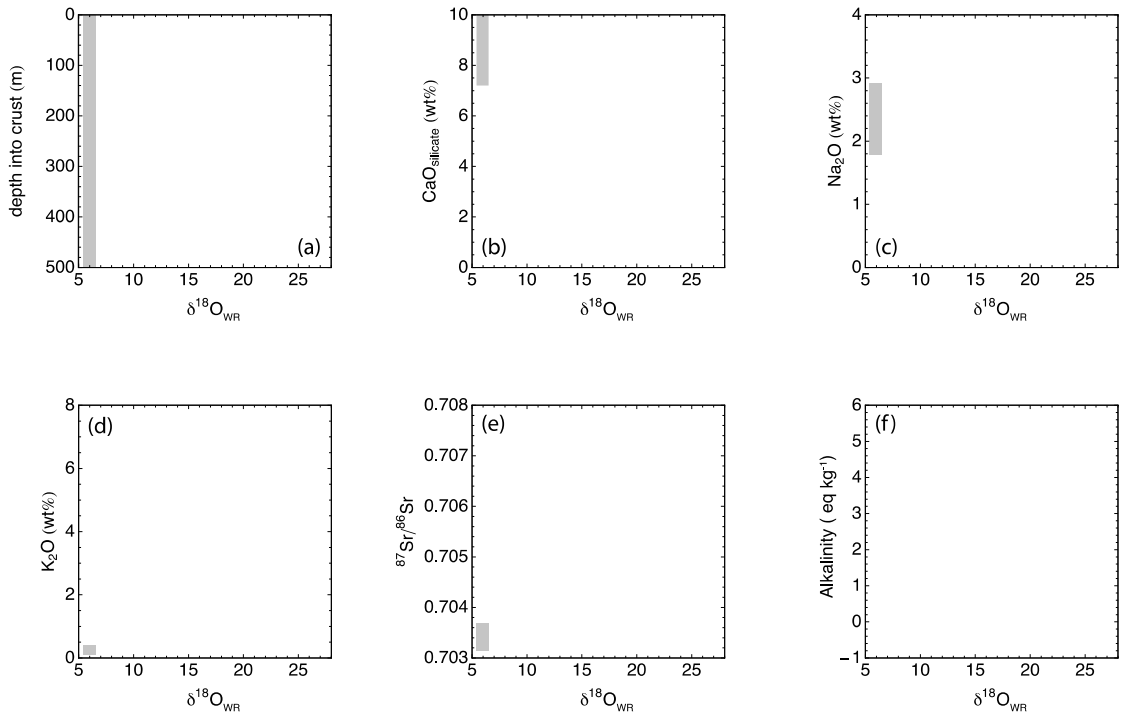

Figure 5. Whole-rock $\delta^{18}O$ ($\delta^{18}O_{WR}$; VSMOW) v (a) depth, (b) CaO_{sil} (the whole-rock CaO content minus the CaO stored in carbonate minerals determined from the whole-rock CO_2 content assuming this is all housed in $CaCO_3$), (c) Na_2O, (d) K_2O, (e) Sr-isotope ratio (age corrected to 87 Myr), and (f) calculated alkalinity produced by fluid rock reaction (Coogan and Gillis, 2018b). Grey boxes show estimated fresh-rock compositions. The different colour symbols represent different sampling areas in the Troodos ophiolite: Green: Mitsero; Blue: Akaki; Orange: Politico; Black: Onophrious (see Fig. S2) and the smaller grey symbols in parts (b) to (e) are composite samples from DSDP Sites 417 and 418 (Staudigel et al., 1996) and ODP Hole 801C (Kelley et al., 2003; Alt, 2003). For Hole 801C the O-isotope data were corrected for intermixed sediment using the data in Alt (2003) and these samples are only shown for Na_2O and

K_2O due to lack of data for other species. Whole-rock $\delta^{18}O$ are higher shallower in the crust and correlate with increased K_2O uptake from seawater, increased CaO and Na_2O release into seawater and increased $^{87}Sr/^{86}Sr$ exchange with seawater. Increased alkalinity production from the major element exchange between the crust and ocean also correlates with increased whole-rock $\delta^{18}O$ because both broadly reflect the extent of rock recrystallization.

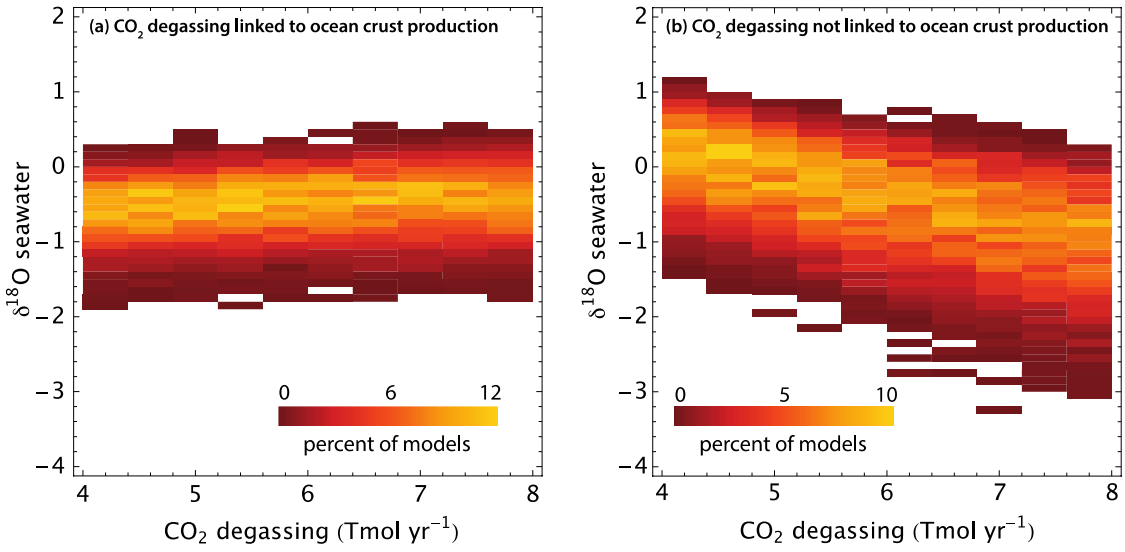

Figure 6. Density plot of the results of Monte Carlo modelling of the steady-state $\delta^{18}O$ of seawater (VSMOW) as a function of changing solid Earth CO_2 degassing rate for the range of parameters given in Table S5. Part (a) has a 1:1 relationship between the rates of CO_2 degassing and oceanic crust formation and part (b) has no relationship between these parameters. The solid earth degassing rate shown is just that portion that is taken up as inorganic C and ignores the ~20% consumed as organic C; i.e. total degassing rates would be higher. For realistic ranges of Phanerozoic CO_2 degassing (as shown) the O-isotopic composition of the ocean (and continental ice) cannot vary much from the modern value if the rate of solid earth CO_2 degassing is tied to the rate of oceanic crustal production (a). If these are not linked, increased CO_2 degassing requires more low-temperature weathering reactions to drawdown the extra CO_2 into rocks and hence removes more ^{18}O from the ocean driving seawater isotopically lighter (b). Colour scale gives percent of model within a given range of $\delta^{18}O_{SW}$ for a given CO_2 degassing rate.

Table

Table 1. Equations used in modelling the O-isotopic composition of seawater

$\frac{d(\delta^{18}\mathrm{O}_{SW})}{dt} = \frac{M_L^O(5.7-\delta^{18}\mathrm{O}_{AL}) + M_D^O(5.7-\delta^{18}\mathrm{O}_{AD}) + M_P^O(5.7-\delta^{18}\mathrm{O}_{AP}) + M_{SS}^O(6-\delta^{18}\mathrm{O}_{SS}) + M_{LM}^O(6-\delta^{18}\mathrm{O}_{LM})}{m_o}$	Eq. S1
$\delta^{18}\mathrm{O}_{AL} = (\delta^{18}\mathrm{O}_{SW} + 30 - 0.25T_{BW})F_{LT} + 5.7(1-F_{LT})$	Eq. S7
$\delta^{18}\mathrm{O}_{AD} = 4.5 + 0.6\delta^{18}\mathrm{O}_{SW}$	Eq. S3
$\delta^{18}\mathrm{O}_{AP} = 5.1 + 0.2(\pm 0.02)\delta^{18}\mathrm{O}_{SW}$	Eq. S4
$\delta^{18}\mathrm{O}_{SS} = (\delta^{18}\mathrm{O}_{SW} - 3) + 20(\pm 2) - 0.25(T_S - 15)$	Eq. S10
$\delta_{LM} = \delta^{18}\mathrm{O}_{SW} + \left(\left(\frac{18030}{T_S+273}\right) - 32.43\right)$	Eq. S11
$F_{LT} = 0.07(\pm 0.02)\mathrm{Exp}\left(\left(\frac{E_a^{SFW}}{R}\right)\left(\frac{1}{275} - \frac{1}{T_{BW}+273}\right)\right)$	Eq. S6
$M_{SS} = 2(\pm 0.3) \times 10^5 \mathrm{Exp}\left(\left(\frac{E_a^{cont}}{R}\right)\left(\frac{1}{288} - \frac{1}{T_S+273}\right)\right)$	Eq. S9
$M_{LM} = M_{SS}/5(\pm 1)$	Eq. S8

M^O: mass of oxygen added to the reservoir per unit time; *L*: lavas in seafloor weathering zone; *AL*: altered lavas; *D*: dikes; *AD*: altered dikes; *P*: plutonic rocks; *AP*: altered plutonic rocks; *SS*: newly formed silicate sediment; *LM*: carbonate sediment derived from silicate weathering; m_o: mass of oxygen in ocean; F_{LT}: fraction of lavas recrystallized during seafloor weathering. Surface temperature (T_S) is set such that sufficient alkalinity is generated via seafloor weathering and continental weathering to draw-down the CO_2 degassing flux prescribed in the model. Bottom water temperature (T_{BW}) = T_S – 11 (Krissansen-Totton and Catling, 2017); E_a: activation energy for seafloor weathering (*SFW*) and continental weathering (*cont*); Equation numbers refer to the supplementary material where these equations are described in detail.